ELSEVIER

Journal of Alloys and Compounds 262–263 (1997) 81–86

Journal of ALLOYS AND COMPOUNDS

XAFS studies of local atomic structure of niobium tellurides

Yves Mathey[a,*], Herve Sassoli[a], Juris Purans[a,b]

[a]*CNRS UMR 6631, Faculté des Sciences de Luminy, Université de la Méditerranée, F-13288 Marseille, Cedex 9, France*
[b]*Institute of Solid State Physics, University of Latvia, LV-1063 Riga, Latvia*

Abstract

We present XAFS (K-edge) studies of the local atomic structure around the Nb and Te ions in niobium tellurides ($NbTe_2$, Nb_3Te_4 and $NbTe_4$) in comparison with $ZrTe_2$. Using a multi-shell best-fit analysis procedure, we have reconstructed local environments of the Nb and Te ions and compared them with the existing structural models. We found that at the Nb K-edge the XAFS data of $NbTe_4$ are extremely sensitive to metal clustering and to the subsequent departure from the average crystallographic positions. Moreover, at Te K-edge the XAFS data allowed us to distinguish the different type of Te–Te bonds, for instance: the dimer (Te–Te: 2.9 Å) and the squares (Te–Te: 3.3 Å) in $NbTe_4$, the interlayer and intralayer (Te–Te: 2.9–4.0 Å) in $NbTe_2$, through their Debye–Waller characteristics. In addition, a comparative analysis of Debye–Waller factors obtained in the different coordination shells (Te–Te, Te–Nb, Nb–Te and Nb–Nb) shows an evidence of correlation in the vibrational motion. © 1997 Elsevier Science S.A.

Keywords: XAFS; Niobium tellurides; Metal clustering

1. Introduction

It is well established, nowadays, that X-ray absorption fine structure (XAFS) may provide additional information to X-ray diffraction (XRD). The local lattice distortion around the ions in crystalline materials near phase transitions, or in solid solutions, or after exchange reaction can be studied from a local point of view, while XRD gives only the average long range lattice structure [1a,b,c]. Many efforts have been devoted to study the structure of low dimensional transition metal 1D and 2D compounds [2–5]. However, relatively little is known about the local order and lattice dynamics in these compounds. In this paper we present the XAFS study of local order of low dimensional (2D, pseudo-1D or modulated-1D) niobium tellurides: $NbTe_2$ [2], Nb_3Te_4 [3], $NbTe_4$ [4] and $ZrTe_2$ [5] (as a non-distorted reference) crystals at low (80 K) and room temperatures.

The aim of this investigation is to show that the lattice distortion around the ions in crystalline tellurides can be probed locally by XAFS and then compared with known XRD average data of the long-range lattice structure. In particular, our low-temperature XAFS studies have shown that niobium ions in $NbTe_4$ crystal exhibit a strong preference for short and long sites, while XRD data of a modulated structure shows a continuous distribution of Nb–Nb and Te–Te distances [4].

2. Experimental

The crystalline compounds were prepared starting from pure niobium (Koch-light, 5 N) and pure tellurium (Fluka, 5 N). In order to prevent oxidation, alloys (approximately 1 g) were formed by direct reaction of the pure elements in a silica tube (~5 mm

---

[*] Corresponding author.

PII S0925-8388(97)00333-2

inside diameter, ~ 6 mm outside diameter, ~ 25 mm length) sealed under vacuum. The sealed ampoule was then put in a furnace and the temperature was slowly raised up to the chosen value (typically 500°C, 550°C and 1000°C for NbTe$_4$, NbTe$_2$ and Nb$_3$Te$_4$, respectively) and was kept at this level for approx. 1 week. The crystalline tellurium was obtained by a slow cooling (0.1 K min^{-1}). The resulting crystalline powders have been checked by X-ray diffraction.

The sample for X-ray absorption measurements was prepared as follows: the crystalline powders were finely ground and the powders were dispersed in methyl alcohol by an ultrasonic mixer and then uniformly deposited on a polytetrafluoroethylene membrane.

The Te K-edge XAFS spectra were measured in transmission mode at the DORIS III storage ring (HASYLAB, Germany) using the Römo II EXAFS station on the beamline X1.1 wiggler beamline. The positron energy was 4.5 GeV with a current of approx. 100 mA. The synchrotron radiation was monochromatized using the Si(311) double-crystal monochromator and its intensity was measured by three ionisation chambers containing krypton gas. The Nb K-edge XAFS spectra were measured in transmission mode at the DCI storage ring (Orsay, France) using the EXAFS-3 station on the D21 bending magnet beam line. The positron energy was 1.8 GeV with a current of approx. 300 mA. The synchrotron radiation was monochromatized using the Si(311) channel-cut crystal monochromators and its intensity was measured by two ionization chambers containing argon.

The experimental Te K-edge spectra were recorded at two different temperatures (80 K and room temperature) in the energy range 31500–33000 eV, with a 3-eV energy step and an energy resolution equal to 10 eV. The Nb K-edge spectra were recorded at two different temperatures (80 K and room temperature) in the energy range 18800–19800 eV, with a 2-eV energy step and an energy resolution equal to 5 eV. Crystalline trigonal t-Te and layered ZrTe$_2$ were used as a reference compounds. Their XAFS were recorded at the same conditions.

3. Results and discussion

The experimental data were analysed by the XAFS data analysis software package 'EDA' [6] implementing the data analysis constraints refinement based on crystallographic data and lattice dynamics models proposed in this work. In the case of K-edge of Nb and Te, E_0 is located near the first inflection point. The experimental XAFS signal $\chi(\kappa)$ was multiplied by a factor κ^2 (see the example of experimental curves in Fig. 1). The Fourier transforms (FT) of the experimental XAFS signals in the range from 1.0 to 16 Å^{-1} are shown in Fig. 2.

The evolution of FTs with temperature (80 K and room temperature) are presented on the same figure. The first peak in the FTs is sharp for low and room temperatures. When the temperature is raised the amplitude of the first-shell peak decreases due to increase of the thermal disorder. As expected, the amplitude of the next shell peaks declines more rapidly. The contributions of first shells atoms up to (4 Å) were singled out by a back FT in the range of 1.5–4.2 Å for the Nb and Te surroundings. The XAFS signal ($k = 2$–15.0 Å^{-1}) thus obtained was utilized in the best fit multi-shell analysis procedure.

The fitting procedure of the XAFS spectra was based on the single-scattering curved-wave formalism. The XAFS signal was calculated using the standard expression (see [6]) where N_i is the coordination number of the ith shell, R_i is the radius of the ith

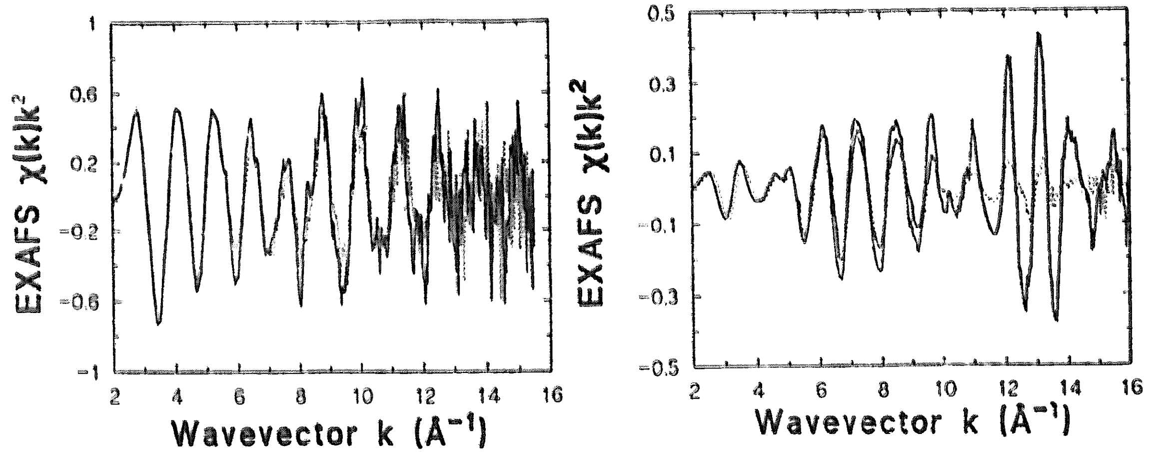

Fig. 1. Experimental XAFS signals at the Nb (left figure) and Te (right figure) K-edges in NbTe$_4$ at low (solid line) and room (dashed line) temperatures.

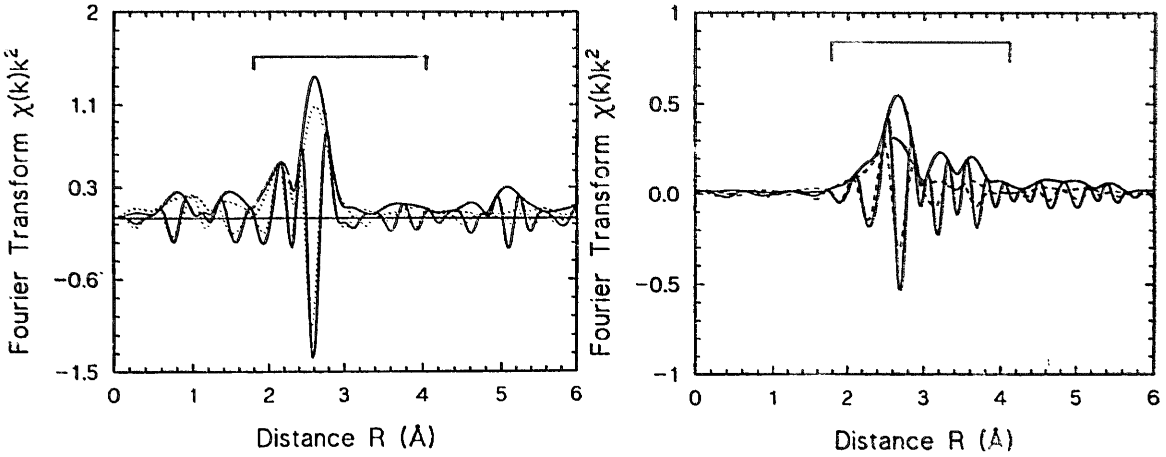

Fig. 2. FTs of the experimental spectrum at the Nb (left figure) and Te (right figure) K-edges in $NbTe_4$ at low (solid line) and RT (dashed line). The modulus and imaginary parts are shown. The range of the back FT is indicated (top solid line).

shell, σ_i^2 is the Debye–Waller (DW) factor. Backscattering amplitudes and phases were calculated by the FEFF6 code [7] for the clusters of 6 Å radii constructed on the crystallographic data of the $NbTe_2$ [2], Nb_3Te_4 [3], $NbTe_4$ [4], $ZrTe_2$ [5] and t-Te [8] crystals.

The importance of single-scattering (SS) and multiple-scattering (MS) contributions were checked using the FEFF6 code. In the niobium telluride compounds the inclusion of MS effects in the analysis up to 4 Å is not important, due to their particular structure with large interatomic distances. Therefore the analysis of FTs up to 4 Å includes only SS contributions.

The maximum number of fitting parameters is limited in general by the number of independent data points $N_{ind} \cong 2\Delta k\Delta R/\pi + 2$ where Δk and ΔR are, respectively, the widths in k and R space used in the fit [9]. In the case of Nb and Te, N_{ind} is approx. 24 ($\Delta k = 13$ and $\Delta R = 2.7$). Thus, if we take three fitting parameters per shell, the maximum numbers of shells which can be used are eight. We used n-shell (two, three and four shell) models (Nb–Te_i and Nb–Nb_i) or (Te–Nb_i and Te–Te_i) with three n-varying parameters and the fitting parameters for each shell were coordination numbers, distances and DW factors.

Based on the fitting parameters, the radial distribution function (RDF) can be reconstructed according to the equation of the sum of Gaussian distributions [6]. This graphical representation (see Figs. 3 and 4 and Ref. [10]) is useful since it takes into account not only coordination numbers and peak positions but also DW factor values (static and dynamic part) and overlap of different shell contributions. In the following section, we will compare our results with possible local structure around possible crystallographic sites of niobium tellurides. The results of the fitting procedure are gathered in Table 1. The values of the fitted parameters are an average of different best fit calculations, and the indicated errors present the possible uncertainties. The experimental and calculated spectra of the reference compounds are also shown in Figs. 3 and 4. The structure of a single layer of a non-distorted CdI_2-type MeX_2 ($ZrTe_2$) is known: the chalcogen and metal atoms form regular hexagons (see Fig. 5 in Ref. [11]) in planes perpendicular to the c axis. In the distorted $NbTe_2$ structure, the metal atoms manifest clustering in the layer with a double zigzag chain formed by short (Nb–Nb_1 approx. 3.3 Å) and long (Nb–Nb_2 approx. 3.6 Å) distances. In the non-distorted $ZrTe_2$ layered structure or in the t-Te (intrachain Te–Te_1 and interchain Te–Te_2 distances), two-shell fit of simple structure gives reasonable results for coordination numbers, distances and DW factors. However, in distorted niobium tellurides the large number of subshells requires a large number of fitting parameters. As a result, parameters in the subshells, and particularly the coordination numbers and DW factors, become highly correlated. To solve this problem we have used a constrained refinement of XAFS data and compared the RDFs reconstructed from XAFS and XRD data.

Usually for the ordered crystalline compounds it was proposed that parameters may be restricted by assuming that only integer values of occupation number are considered and that all similar type of atoms at similar distances have the same DW factor [12]. However, the layered 2D crystals as TM dichalcogenides must have very different DW factors between intralayer and interlayer atoms. We have therefore associated the interlayer and intralayer atoms in the independent subshells with different DW factors. For example the second coordination shell of $ZrTe_2$ has three types of Te–Te distances (see Fig. 5 in Ref. [11]): six intralayer distances at 3.950 Å in the same plane of the $ZrTe_2$ layer; three intralayer distances at

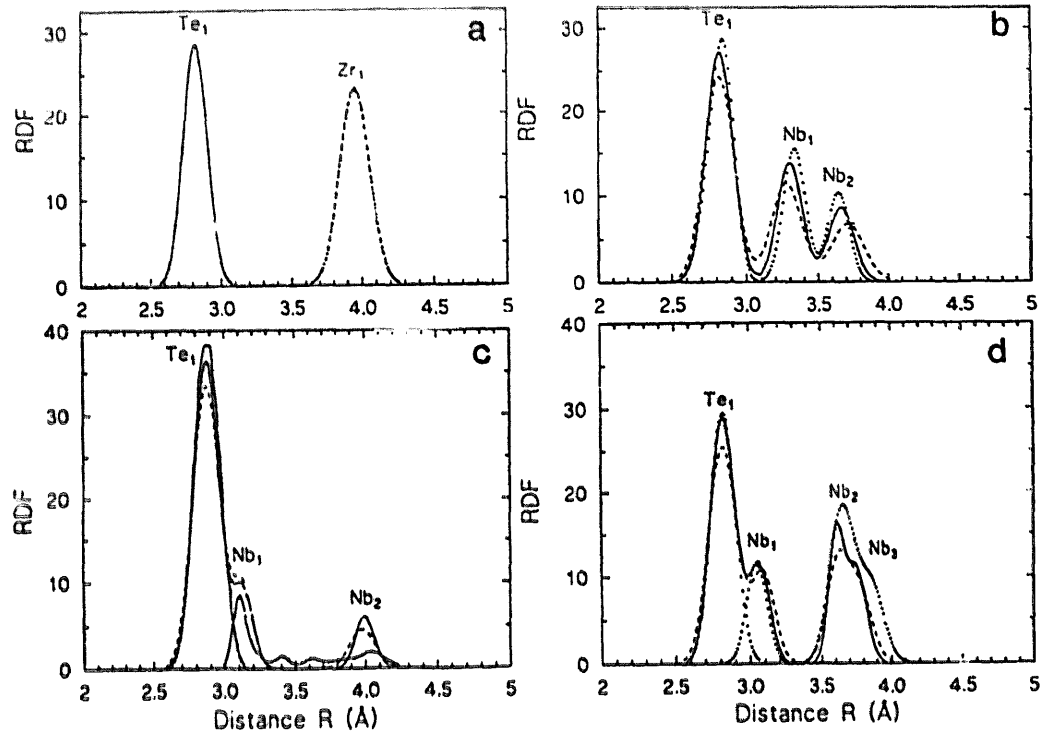

Fig. 3. Comparison of the RDFs of ZrTe$_2$ (a), NbTe$_2$ (b), NbTe$_4$ (c) and Nb$_3$Te$_4$ (d) reconstructed from the Me K-edge XAFS data fitting results at low (solid line) and room (dashed line) temperatures of this work (see Table 1) with RDFs corresponding to XRD crystallographic data (dotted line). The continuous distribution of Nb–Nb distances calculated from XRD data (full line) is also shown for the incommensurate NbTe$_4$ structure.

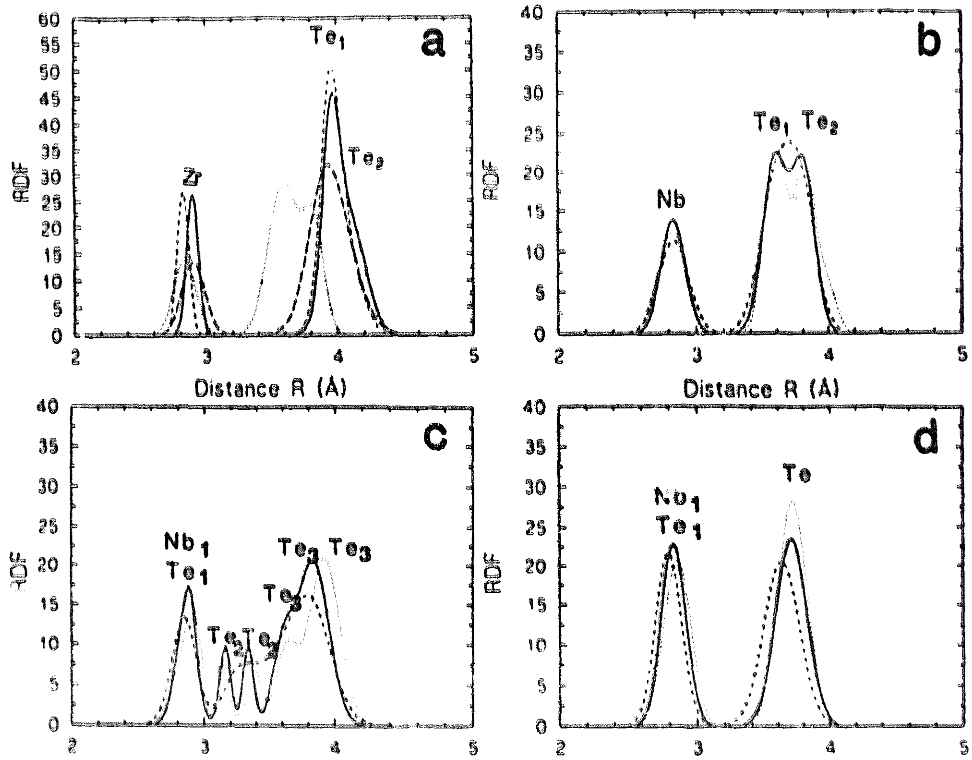

Fig. 4. Comparison of the RDFs of ZrTe$_2$ (a), NbTe$_2$ (b), NbTe$_4$ (c) and Nb$_3$Te$_4$ (d) reconstructed from Te K-edge EXAFS data fitting results at low (solid line) and room (dashed line) temperatures of this work (see Table 1) with RDFs corresponding to XRD crystallographic data (dotted line).

Table 1
Structural data obtained from the best-fit analysis of the Me and Te K-edge XAFS in Me$_x$Te$_y$ compounds

Crystals Me edge	Me–Te$_1$			Me–Me$_2$ and Me–Te$_2$			ϵ($\times 10^{-3}$)
	N_1	R_1 (Å)	σ_1^2 (Å^2)	N_2	R_2 (Å)	σ_2^2 (Å^2)	
NbTe$_2$ LT	6.0 (Te)	2.825	0.0078	3.0 (Nb)	3.301	0.0088	1.4
				2.0 (Nb)	3.649	0.009	
NbTe$_2$ RT	6.0 (Te)	2.819	0.0098	3.0 (Nb)	3.279	0.0125	1.3
				2.0 (Nb)	3.657	0.0227	
Nb$_3$Te$_4$ LT	6.0 (Te)	2.820	0.0067	2.0 (Nb)	3.045	0.0051	3.2
				2.0 (Nb)	3.595	0.0070	
				2.0 (Nb)	3.728	0.0161	
Nb$_3$Te$_4$ RT	6.0 (Te)	2.819	0.0088	2.0 (Nb)	3.069	0.0064	1.1
				2.0 (Nb)	3.602	0.0078	
				2.0 (Nb)	3.778	0.0117	
NbTe$_4$ LT	8.0 (Te)	2.876	0.0082	1.0 (Nb)	3.133	0.0050	2.6
				1.0 (Nb)	3.934	0.0060	
NbTe$_4$ RT	8.0 (Te)	2.875	0.0091	1.65 (Nb)	3.127	0.0048	2.3
				0.0 (Nb)	—	—	
ZrTe$_2$ RT	6.0 (Te)	2.884	0.0062	6.0(Zr)	3.950	0.0107	0.4
Te edge	Te–Me$_1$ and Te–Te$_1$			Te–Me$_2$ and Te–Te$_2$			ϵ($\times 10^{-3}$)
	N_1	R_1 (Å)	σ_1^2 (Å^2)	N_2	R_2 (Å)	σ_2^2 (Å^2)	
NbTe$_2$ LT	3.0 (Nb)	2.833	0.0075	5.0 (Te)	3.583	0.0086	0.8
				4.5 (Te)	3.802	0.0076	
NbTe$_2$ RT	3.0 (Nb)	2.836	0.0112	5.0 (Te)	3.609	0.018	0.8
				4.5 (Te)	3.820	0.011	
Nb$_3$Te$_4$ LT	4.3 (Nb)	2.828	0.0071	10.0 (Te)	3.709	0.016	3.8
Nb$_3$Te$_4$ RT	3.2 (Nb)	2.793	0.0066	10.0 (Te)	3.680	0.022	3.1
NbTe$_4$ LT	2.0 (Nb)	2.847	0.0045	2.0 (Te)	3.608	0.0070	1.8
	1.0 (Te)	2.887	0.0019	6.0 (Te)	3.837	0.0136	
	1.0 (Te)	3.159	0.0017				
	1.0 (Te)	3.335	0.0017				
NbTe$_4$ RT	2.0 (Nb)	2.829	0.0090	2.0 (Te)	3.530	0.020	1.3
	1.0 (Te)	2.875	0.0052	6.0 (Te)	3.809	0.024	
	2.0 (Te)	3.256	0.0153				
ZrTe$_2$ LT	3.0 (Zr)	2.892	0.0021	12.0 (Te)	3.960	0.0090	2.4
ZrTe$_2$ RT	3.0 (Zr)	2.897	0.0076	12.0 (Te)	3.925	0.0197	1.0

N_i is the number of Me or Te atoms located in the ith shell at distance R from the Me (± 0.02 Å) or Te (± 0.02 Å); σ^2 is the DW factor (± 0.002 Å^2); ϵ is the fitting error.

4.023 Å towards the opposite side of the layer; and three interlayer (or 'through-gap') distances also at 4.023 Å. Consequently three subshell fit of XAFS data must be done.

Moreover, distorted structures such as NbTe$_2$ or Nb$_3$Te$_4$ contain many distances in one subshell and therefore the obtained DW factors have static and dynamic contributions. In order to circumvent the problem of averaging of many contributions in one subshell, the RDFs are simulated with all interatomic distances and coordination numbers obtained from crystallographic (XRD) data and upon adjusting the DW factors only.

In such a way, the reconstructed RDFs from the XAFS data were compared (see Figs. 3 and 4) with those obtained from the crystallographic XRD data. As a result, the structural disorder (set or continuous distribution of distances) and thermal (vibrational) disorder were quantitatively taken into account.

In NbTe$_2$, for instance, we have started the fit of the Nb–Nb second shell with a two-shell model taking into account the short pair Nb–Nb$_1$ and the long pair Nb–Nb$_2$ with four fitting parameters (distances and DW factors). The results (see Table 1) demonstrate the high sensitivity of this second coordination shell to the metal atom clustering phenomena. In this last compound also, a shortening of the c axis and a narrowing of the interlayer slabs has been evidenced. The obtained DW factors of Me–Te$_1$ and Te–Me$_1$ pairs show different behaviour due to the different contributions of the subshells. The DW factors of Me–Te$_1$, at low temperature are approx. 0.007 Å^2 and increase with the temperature only up to 0.001 Å^2 value at room temperature. Therefore the many contributions to the DW at low temperature give non-resolved subshells. On the contrary, in the highly symmetric 2D $ZrTe_2$ the thermal disorder gives the main contribution to the DW factors. For Nb_3Te_4 a three shell model was also tested varying only distances and DW factors.

Also Te and Nb K-edge XAFS data of $NbTe_4$ (see structure in Fig. 5 of Ref. [4]) were fitted by constrained refinement analysis. The dimers of tellurium atoms ($Te-Te_1$ approx. 2.91 Å) are arranged in infinite two-dimensional nets of squares ($Te-Te_2$ 3.29 Å). The metal atoms are located between tellurium squares (between the layers). Short ($Nb-Nb_1$ approx. 3.12 Å) and long ($Nb-Nb_1$ approx. 3.42 Å) metal–metal bonds were observed in the distorted one-dimensional metal chain [4]. Therefore, the two first Te–Te shells (intralayer $Te-Te_1$ 2.91 Å arranged in the infinite two-dimensional nets of squares $Te-Te_2$ 3.29 Å) must have very small DW factors, while the next two Te–Te shells (interlayer distances) must have significantly higher DW factors. The first shell $Te-Nb_1$, $Nb-Te_1$, as well as the second shell $Nb-Nb_1$ and $Nb-Nb_2$ DW factors (static part) must significantly depend on the rearrangement of metal atoms in a one-dimensional chain due to the modulation of $NbTe_4$ structure.

We have compared (see Fig. 3c) our XAFS results (80 K) with a model of clustering (only short and long distances of the modulated structure [4]) on the one hand and with a model of continuous distribution along the chain (see Fig. 5 in Ref. [4] = second harmonic modulated structure) on the other. For that purpose we have calculated the RDFs within these two models using the XRD data [4]. This comparison agrees better with the clustering model and the obtained $Nb-Nb_1$ and $Nb-Nb_2$ distances are in good agreement with the XRD data of this model.

We suggest therefore that, at low temperature, due to the decrease of the DW factors, the high order modulation waves became more important. It is clear that the remarkable narrowness in the reconstructed RDF of $NbTe_4$ at low temperature reflects a strong temperature sensitivity of these DW factors; it brings also an evidence of correlation in the vibrational motion due to the particular intra/interchain dynamics.

4. Conclusions

Upon conjugating low temperature and large wavevector range exploration, it turns out to be possible to obtain well resolved radial distribution functions (RDFs) reconstructed from the experimental data fitting results. The local environments obtained are built on exclusive constrained model of coordination numbers (known from crystallographic data). The corresponding distances are in a good agreement with the crystallographic data for distorted and 'metal clustered' $NbTe_2$ and Nb_3Te_4 structures. For the so-called 1D modulated $NbTe_4$ compound, XAFS data show a good agreement with the clustering model. In particular, while XRD data of the second order modulated structure have led us to propose a continuous distribution of Nb–Nb and Te–Te distances, our low-temperature XAFS studies have shown that niobium ions in $NbTe_4$ crystal exhibit a strong preference for short and long sites. We propose, therefore, that an intrachain local chemical order (Nb–Nb clustering) exists in the $NbTe_4$ compound at low temperature.

References

[1a] P.A. O'Day, J.J. Rehr, S.I. Zabinsky, G.E. Brown, Jr., J. Am. Chem. Soc. 116 (1994) 2938.
[1b] A. Kuzmin, N. Mironova, J. Purans, A. Rodionov, J. Phys. Condens. Matter 7 (1995) 9357.
[1c] F. Rocca, A. Kuzmin, J. Purans, G. Mariotto, Phys. Rev. B 50 (1994) 6662.
[2] B.E. Brown, Acta Crystallogr. 20 (1966) 264.
[3] K. Selte, A. Kjekshus, Acta Crystallogr. 17 (1964) 1568.
[4] S. van Smaalen, K.D. Bronsema, J. Mahy, Acta Crystallogr. B 42 (1986) 43.
[5] F. Lévy (Ed.), Crystallography and Crystal Chemistry of Materials with Layered Structures, Reidel, Dordrecht, Holland, 1976.
[6] A. Kuzmin, Physica B 208/209 (1995) 175.
[7] J.J. Rehr, J. Muster de Leon, S.I. Zabinsky, R.C. Albers, J. Am. Chem. Soc. 113 (1991) 5135.
[8] C. Andenis, V. Langer, O. Linqvist, Acta. Crystallogr. C45 (1989) 941.
[9] Report on the International Workshop on Standards and Criteria in XAFS, in: Hasnain S.S. (Ed.), X-Ray Absorption Fine Structure, Ellis Horwood, New York, 1991, p. 751.
[10] Y. Mathey, J. Purans, H. Sassoli, in: Soleil de l'Arc Méditerranéen, Marseille, Nov., 1995 (Les Editions de Physique, 1997).
[11] E. Canadell, S. Jobic, R. Brec, J. Rouxel, M.-H. Whangbo, J. Solid State Chem. 99 (1992) 189.
[12] M.C. Co, K.O. Hodgson, J. Am. Chem. Soc. 103 (1981) 3200.